35th Annual International Conference of the IEEE EMBS
Osaka, Japan, 3 - 7 July, 2013

Automated Microaneurysm Detection Method Based on Eigenvalue Analysis Using Hessian Matrix in Retinal Fundus Images

Tsuyoshi Inoue, Yuji Hatanaka, *Member, IEEE*, Susumu Okumura
Chisako Muramatsu, and Hiroshi Fujita, *Member, IEEE*

Abstract— **Diabetic retinopathy (DR) is the most frequent cause of blindness. Microaneurysm (MA) is an early symptom of DR. Therefore, the detection of MA is important for the early detection of DR. We have proposed an automated MA detection method based on double-ring filter, but it has given many false positives. In this paper, we propose an MA detection method based on eigenvalue analysis using a Hessian matrix, with an aim to improve MA detection. After image preprocessing, the MA candidate regions were detected by eigenvalue analysis using the Hessian matrix in green-channeled retinal fundus images. Then, 126 features were calculated for each candidate region. By a threshold operation based on feature analysis, false positive candidates were removed. The candidate regions were then classified either as MA or false positive using artificial neural networks (ANN) based on principal component analysis (PCA). The 126 features were reduced to 25 components by PCA, and were then inputted to ANN. When the method was evaluated on visible MAs using 25 retinal images from the retinopathy online challenge (ROC) database, the true positive rate was 73%, with eight false positives per image.**

I. Introduction

In Japan, the number of diabetic patients tends to increase. According to the Ministry of Health, Labour and Welfare in Japan, it has been estimated that there are approximately nine million people with diabetes and approximately 22 million people with suspected diabetes. Diabetic retinopathy (DR) is a complication of diabetes and may cause blindness. Visual loss can be prevented by early detection and treatment of DR. However, it is difficult for patients to notice DR, because it progresses without subjective symptoms. Ophthalmologists can detect DR by finding microaneurysm (MA), hemorrhage, exudate, or neovascularization in the retinal fundus. In this study, our purpose is to develop an automatic MA detection method. Because MA is an early symptom of DR, MA detection can enable early detection of DR.

In 2009, the retinopathy online challenge (ROC) was held in order to compete for MA detection performance using the same retinal fundus images [1]. Several study results have been reported since the contest. Niemijer et al., the organizers of the ROC, proposed an MA detection method based on morphological top-hat transform and pixel classification. Afterward, the results were combined and the candidates were classified by the k-nearest neighbor algorithm [2]. Sanchez et al. proposed a detection method based on logistic regression [3]. Cree et al. proposed a detection method based on top-hat transform and a Bayes classifier [4]. Quellec et al. proposed a method based on template matching using wavelet transform [5]. Zhang et al. proposed a method based on a multiscale Gaussian correlation filter and space representation classifier [6, 7]. Antal et al. proposed a detection method based on ensemble learning [8, 9]. This last method was judged to be the optimum combination of the preprocessing method and the MA detection method. Lazar et al. proposed a detection method based on profile analysis at multiple angles [10]. Fegyver et al. proposed a method based on analysis of the concentration gradient [11]. Giancardo et al. proposed a detection method based on the Radon transform [12].

Several study results outside ROC have also been reported. Sopharak et al. proposed a detection method based on extended-minima transform and a naive Bayes classifier [13, 14]. Purwaita et al. proposed a detection method based on edge extraction [15].

Using the test images in ROC database, the true positive rate of a human expert was about 49% with 1.08 false positive per image [1]. However, method that has a better performance than a human expert has not been proposed yet. MA detection is very difficult because MA diameter was a tens μm.

We, on other hand, proposed an MA detection method using double-ring filter [16] in the contest. We then proposed false positive deletion method based on texture analysis [17]. Here, a co-occurrence matrix, differential statistics, and a run length matrix were used. However, it had a problem in that many MAs were lost, although the performance of the double-ring filter had peaked. Typical MA also has a pixel value distribution of concave in all directions. We attempted MA detection using eigenvalue analysis of the Hessian matrix as an alternative approach in order to detect such regions and evaluated the effectiveness of the method.

II. Method

In this study, images from the ROC database were used. The ROC database comprises 50 training images and 50 test images, each with three different resolutions. The ROC database was created to evaluate the different proposed methods. On the ROC website, the results for 12 groups have been reported. In the training images, the gold standard for MA, determined by four ophthalmologists, was given.

This work was supported in part by Grant-in-Aid for Young Scientists (B) from The Ministry of Education, Culture, Sports, Science and Technology, Japan.

T. Inoue is a graduate student in the Division of Electronic Systems Engineering, Graduate School of Engineering, the University of Shiga Prefecture, 2500 Hassaka-cho, Hikone-shi, Shiga 522-8533, Japan (phone: 81-749-28-9556; e-mail: ze23tinoue@ec.usp.ac.jp).

Y. Hatanaka and S. Okumura are with the Department of Electronic Systems Engineering, School of Engineering, the University of Shiga Prefecture, 2500 Hassaka-cho, Hikone-shi, Shiga 522-8533, Japan (phone: 81-749-28-9556; fax: 81-749-28-9576; e-mail: hatanaka.y@usp.ac.jp).

C. Muramatsu and H. Fujita are with the Department of Intelligent Image Information, Graduate School of Medicine, Gifu University, 1-1 Yanagido, Gifu-shi, Gifu 501-1194, Japan.

However, in the test images, the gold standard was not given. We therefore selected 25 training images of approximately 1389 × 1383 pixels [1]. There are 156 MAs and 136 hemorrhages in 25 retinal fundus images, all images including at least one MA or hemorrhage.

A. Overall Scheme for Detection of Microaneurysm

MA appears as a dark spot in the retinal fundus images as shown in Fig. 1. MA diameters are a few pixels in the retinal fundus images.

The flow chart of the overall scheme is shown in Fig. 2. There are differences in brightness and contrast in the retinal fundus images. In order to reduce the adverse effect on image processing because of these differences, we applied brightness correction, gamma correction, and contrast enhancement as preprocessing. The contrast between the MA and retinal area is highest in the green-channel of the color image, so we obtained the green-channel component of the color image for the blood vessel extraction and MA detection. To reduce noise, we applied a low-pass filter based on fast Fourier transform to the green-channel components. This image was applied in the subsequent processes.

To exclude the blood vessels from the candidate regions of MA, we deleted them by combining a double-ring filter and black-top-hat transform [17].

Further, we detected the MA candidate regions by using eigenvalue analysis based on a Hessian matrix. Here, the MA candidate regions were decided by prior processing. MA candidates were modified in the regions by rethresholding the eigenvalue in the Hessian matrix, because the size of the candidate region detected by the previous step was different from its actual size.

The MA candidate regions included many false positives. The candidates were therefore classified into MAs and false positives by using feature analysis and artificial neural network (ANN). In this step, 126 features based on pixel value, shape, and texture analysis were calculated in each of the candidate regions [17]. The typical false positives were then removed by thresholding the feature values. To simplify the ANN model, the set of 126 features was reduced using principal component analysis (PCA), and then inputted to the ANN. ANN was a three-layered network and was learned by using a back-propagation method.

B. Eigenvalue Analysis Using Hessian Matrix

The Hessian matrix is a square matrix of second order partial differentiation derived functions. We attempted to detect MA candidate regions by eigenvalue analysis using a Hessian matrix. When the intensity curve surface of the image can be approximated by the function, the Hessian matrix is given as

$$H(x,y)=\begin{bmatrix}L_{xx}(x,y) & L_{xy}(x,y)\\ L_{yx}(x,y) & L_{yy}(x,y)\end{bmatrix}$$

$$L_{xx}(x,y)=G_{xx}(x,y)*I(x,y)$$

$$L_{xy}(x,y)=G_{xy}(x,y)*I(x,y)$$

$$L_{yx}(x,y)=G_{yx}(x,y)*I(x,y)$$

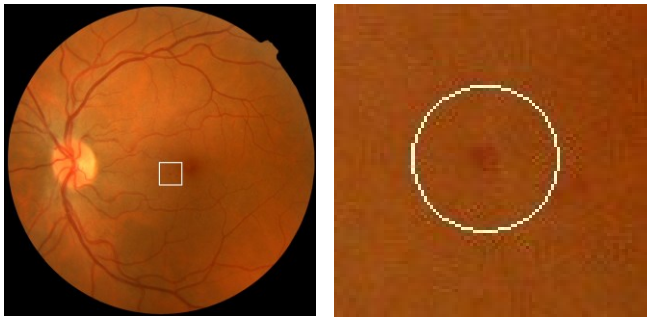

(a) (b)

Figure 1. Example of retinal fundus images with a microaneurysm. (a) Original retinal fundus image, and (b) enlarged view of white box in image (a). There is microaneurysm in center of the image (b)

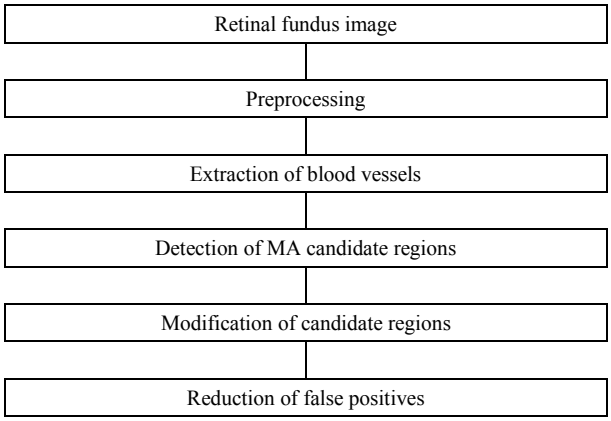

Figure 2. The flow chart of the overall scheme.

$$L_{yy}(x,y)=G_{yy}(x,y)*I(x,y)$$

where $*$ is the convolution operator, $I(x,y)$ is the preprocessed image, and $G_{xx}(x,y)$, $G_{xy}(x,y)$, $G_{yx}(x,y)$, and $G_{yy}(x,y)$ are second order partial derivative functions of the Gaussian function $G(x,y)$ in each direction. The Gaussian function $G(x,y)$ is

$$G(x,y)=\frac{1}{2\pi\sigma^2}\exp\left(-\frac{x^2+y^2}{2\sigma^2}\right)$$

where σ is a parameter to determine the scale of the Gaussian function. In this study, σ is 3.0 and the convolution area is a square region within 3 σ of the pixel of interest.

With the first two eigenvalues of the Hessian matrix, it is possible to classify the shape of the intensity curve surface. The shape index is the classification index. By using two eigenvalues ($\lambda_1 \geq \lambda_2$), the shape index S is given by

$$S=\begin{cases}-\frac{2}{\pi}\arctan\left(\frac{\lambda_1+\lambda_2}{\lambda_1-\lambda_2}\right) & \text{if } \lambda_1 \neq \lambda_2\\ -1 & \text{if } \lambda_1=\lambda_2>0\\ 1 & \text{if } \lambda_1=\lambda_2<0\end{cases}$$

where S is $-1 \leq S \leq 1$. When S has a small value, the possibility of MA is high. However, each eigenvalue in the MA regions was different, and thus many false positives in the particular images were detected when we used a fixed

threshold. To equalize the performance of each image, we limited the number of the candidates detected to 120 per image.

III. RESULT AND DISCUSSION

A. Evaluation Method

The ROC database includes many MAs that are very difficult to detect because of low contrast between the MA and the surrounding retinal area. Therefore, MAs were classified as visible or invisible by consensus of the two engineering researchers in this study. As a result, 85 MAs were classified as visible and 71 as invisible. A visible MA and an invisible MA in the green-channel components are shown Figs. 3(a) and 3(b), respectively. As it is not possible to visually detect invisible MAs, we focused on the detection of visible MAs in this study. If the center of the detected MA existed within the circle of the "gold standard," detection of such an MA was considered as a success.

Using 25 training images, we decided on a maximum number of MA candidates per image, and the threshold values of the 126 features. We then evaluated the final false positive reduction step on the basis of the ANN by the leave-one-out cross validation.

B. Experiment Result

The proposed method and the previous one [17] were evaluated by free-response receiver operating characteristic (FROC) analysis, using output values from the ANN, when the visible MAs or all MAs were set as the detection targets. FROC curves are shown in Fig. 4. Fig. 4 shows that the true positive rate of the proposed method was better than that of the previous one, which had over two false positives per image. TABLE I shows the true positive rates using the proposed method and previous one, when there were eight false positives per image. Fig. 5 shows the examples in the vicinity of an MA, which are the original retinal fundus image, the green-channel component, the image generated by using the values of the shape index *S*, and the image generated by using the output values from the double-ring filter. The MA image was emphasized by the proposed method and the previous one in Figs. 5 (c) and (d), respectively. The double-ring filter uses the pixel value of the pixel of interest and the surrounding pixel values. If the contrast between MA candidate and the retinal area is high, the output of the double-ring filter is low. Thus, the double-ring filter responded to the contrast. However, the filter also emphasized the irregularly shaped spot with high contrast. Fig. 6 shows the example of the false positive mis-detected by previous method. Previous method emphasized the normal region, but proposed method did not emphasize that region. There were normal regions with slight contrast in retinal area. Thus, many false positives were mis-detected. On the other hand, the shape index of the proposed method can classify the shape of the intensity curve surface, i.e., the classification of cup and rut is possible. For this reason, the number of false positives using the proposed method was smaller than that for the double-ring filter. Hence, the proposed method is effective in detecting dark lesion in the retinal fundus image. The proposed method also detected some of the hemorrhages, which were not detection targets in this study. Thus, we did not count the number of hemorrhages detected as false positives.

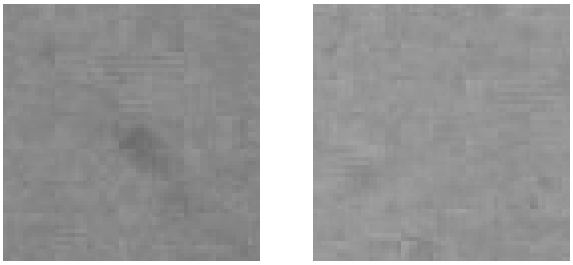

(a) (b)

Figure 3. Example of microaneurysm in green-channel components. (a) green-channel components of visible microaneurysm and (b) green-channel components of invisible microaneurysms. There are microaneurysms in centers of these images.

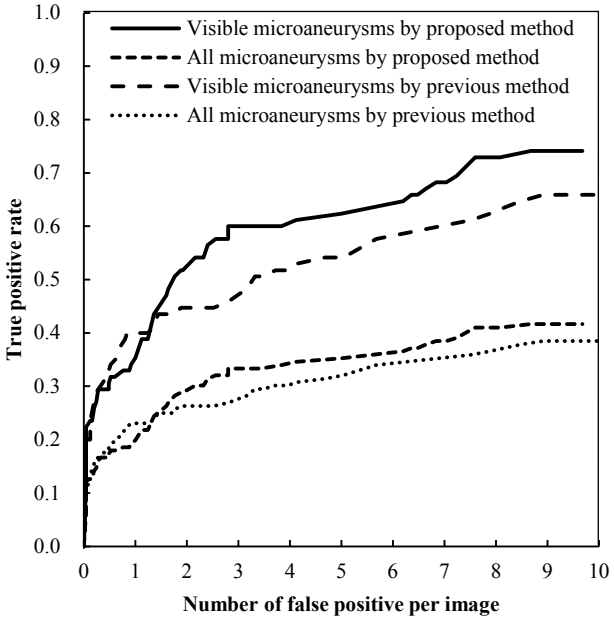

Figure 4. FROC curves for all microaneurysms and only visible microaneurysms.

TABLE I. EXPERIMENT RESULT

	TPR of all microaneurysm	TPR of visible microaneurysm	FPI
Proposed method	0.410(64/156)	0.729(62/85)	8(200/25)
Previous method	0.372(58/156)	0.635(54/85)	8(200/25)

True positive rate (TPR) and the number of false positive per image (FPI) after false positive reduction using threshold operation based on future analysis and artificial neural network.

By changing the scale parameter σ, the proposed method could detect the same MAs. However, some detected MAs by double-ring filter were not detected by the proposed method. We plan to develop the MA detection method by using eigenvalue analysis based on a Hessian matrix combined with a double-ring filter.

IV. CONCLUSIONS

We have developed an MA detection method based on eigenvalue analysis of the Hessian matrix. The proposed method was effective in the detection of dark lesion in the

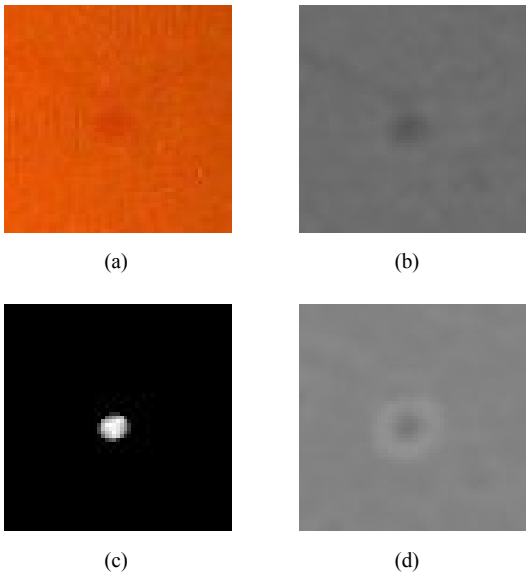

Figure 5. The result of microaneurysm detection. (a) Original retinal fundus image. (b) Preprocessed image. (c) Eigenvalue analysis results (proposed method). Here, if $S = -1$, pixel value is 255, and if $S \geq 0$, pixel value is 0. Otherwise, pixel value is $-S \times 255$. (d) Output image of double-ring filter (previous method).

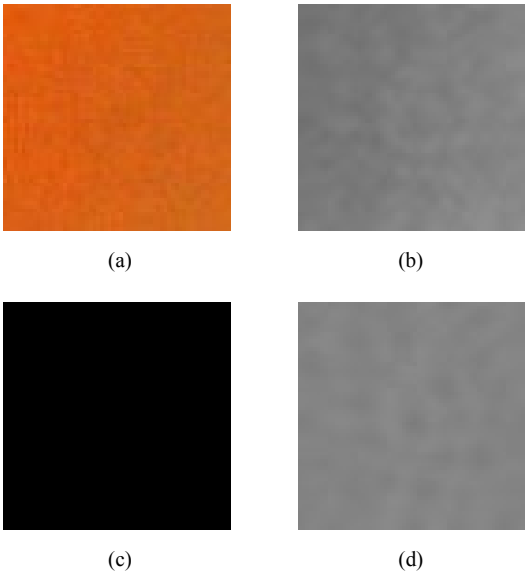

Figure 6. The example of region missed by previous method. (a) Original retinal fundus image. (b) Preprocessed image. (c) Eigenvalue analysis results. (d) Emphasized image by double-ring filter.

retinal fundus image. When this method was evaluated by using 25 training images selected from the ROC database, the true positive rate of visible MAs was 73% at eight false positives per image. For the early detection of diabetic retinopathy, we will need further improvement.

ACKNOWLEDGMENT

The authors thank the school of engineering researchers in the Computer Engineering Laboratory in the University of Shiga Prefecture, and Atushi Mizutani, graduate of Gifu University Graduate School.

REFERENCES

[1] M. Niemeijer, B. van Ginneken, M. J. Cree, A. Mizutani, G. Quellec, C. I. Sanchez, B. Zhang, R. Hornero, M. Lamard, C. Muramatsu, X. Wu, G. Cazuguel, J. You, A. Mayo, Q. Li, Y. Hatanaka, B. Cochener, C. Roux, F. Karray, M. Garcia, H. Fujita, and M. D. Abramoff, "Retinopathy online challenge: automatic detection of microaneurysms in digital color fundus photographs," *IEEE Trans. Medical Imaging*, vol. 29, no. 1, pp. 185–195, Jan. 2010.

[2] M. Niemeijer, B. van Ginneken, J. Staal, M. S. A. Suttorp-Schulten, and M. D. Abramoff, "Automatic detection of red lesions in digital color fundus photographs," *IEEE Trans. Medical Imaging*, vol. 24, no. 5, pp. 584–592, May 2005.

[3] C. I. Sanchez, R. Hornero, A. Mayo, and M. Garcia, "Mixture model-based clustering and logistic regression for automatic detection of microaneurysms in retinal images," *Proc. SPIE Medical Imaging*, vol. 7260, pp.72601M-1-8, 2009.

[4] M.J. Cree, The Waikato Microaneurysm Detector Univ. Waikato, Tech. Rep., 2008 [online]. Available: http://roc.healthcare.uiowa.edu/results/documentation/waikato.pdf

[5] G. Quellec, M. Lamard, P. M. Josselin, G. Cazuguel, B. Cochener, and C. Roux, "Optimal wavelet transform for the detection of microaneurysms in retina photographs," *IEEE Trans. Medical Imaging*, vol. 27, no. 9, pp. 1230–1241, Sep. 2008.

[6] B. Zhang, X. Wu, J. You, Q. Li, and F. Karray, "Hierarchical detection of red lesions in retinal images by multiscale correlation filtering," *Proc. SPIE Medical Imaging*, vol. 7260, no.72601L-1-8, 2009.

[7] B. Zhang, F. Karray, Q.Li, and L. Zhang, "Sparse representation classifier for microaneurysm detection and retinal blood vessel extraction," *Information Sciences*, vol. 200, pp. 78–90, Oct. 2012.

[8] B. Antal, A. Hajdu, "An ensemble-based system for microaneurysm detection and diabetic retinopathy grading," *IEEE Trans. Biomedical Engineering*, vol. 59, no. 6, pp. 1720–1726, June 2012.

[9] B. Antal, I. Lazar, and A. Hajdu, "An adaptive weighting approach for ensemble-based detection of microaneurysms in color fundus images," *Proc. 34th IEEE Engineering in Medicine and Biology Society*, pp. 5955–5958, Aug. 2012.

[10] I. Lazar, and A. Hajdu, "Microaneurysm detection in retinal images using a rotating cross-section based model," *Proc. 8th IEEE International Symposium on Biomedical Imaging*, pp. 1405–1409, Mar. 2011.

[11] Z. Fegyver, A gradient based microaneurysm detector, Tech. Rep., [Online]. Available: http://roc.healthcare.uiowa.edu/results/documentation/zfegyer.pdf

[12] L. Giancardo, F. Meriaudeau, T. P. Karnowski, Y. Li, K. W. Tobin, and E. Chaum, "Microaneurysm detection with radon transform-based classification on retina images," *Proc. 33rd IEEE Engineering in Medicine and Biology Society*, pp.5939–5942, Aug. 2011.

[13] A. Sopharak, B. Uyyanonvara, S. Barman, and T. Williamson, "Automatic microaneurysm detection from non-dilated diabetic retinopathy retinal images," *Proc. World Congress on Engineering 2011*, vol.2, pp. 1583–1586, July 2011.

[14] A. Sopharak, B. Uyyanonvara, and S. Barman, "Fine microaneurysm detection from non-dilated diabetic retinopathy retinal images using a hybrid approach," *Proc. World Congress on Engineering 2012*, vol.2, pp.1207–1210, July 2012.

[15] A. A. Purwita, K. Adityowibowo, A. Dameitry, M. W. S. Atman, "Automated microaneurysm detection using mathematical morphology," *Proc. 2011 International Conference on Instrumentation, Communication, Information Technology and Biomedical Engineering*, pp. 117–120, Nov. 2011.

[16] A. Mizutani, C. Muramatsu, Y. Hatanaka, S. Suemori, T. Hara, and H. Fujita, "Automated microaneurysm detection method based on double-ring filter in retinal fundus images," *Proc. SPIE Medical Imaging*, vol. 7260, pp.72601N-1-8, 2009.

[17] Y. Hatanaka, T. Inoue, S. Okumura, C. Muramatsu, and H. Fujita, "Automated microaneurysm detection method based on double-ring filter and feature analysis in retinal fundus images," *Proc. 25th IEEE International Symposium on Computer-Based Medical Systems*, paper#150, June 2012.